Development of a coupled 1D heat-mass transfer solver for porous solid materials for FDS

Aalto-yliopisto
Insinööritieteiden korkeakoulu

Christian Riitamaa

23.11.2021

1. Background

1. Background

- Increase in hydrogen and battery powered vehicles in the near future
- Current design guides and models may not consider phenomena such as jet flames
- Accidents in tunnels of particular concern
- Tunnel linings: high moisture content, low permeability concrete -> higher spalling risk
- New tools needed for more accurate modelling of tunnel fires
- Joint doctoral project between Aalto University and DTU

1. Background

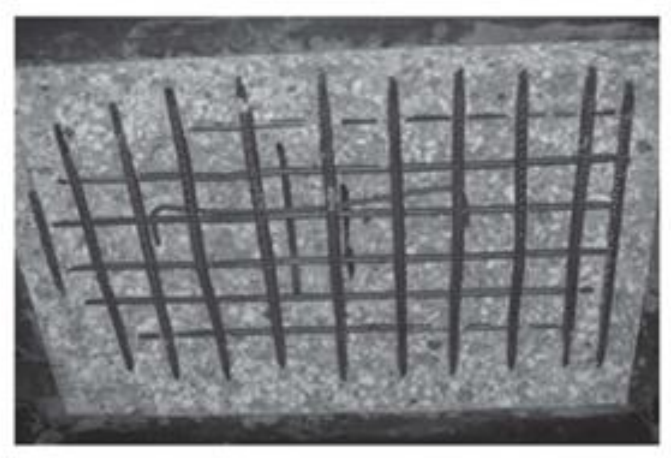

Figure 1. Reinforcement exposed by explosive spalling (left) and the fire-damaged concrete floor of the Liverpool Echo Arena parking garage (31.12.2017) (right)

1. Background

Pressure build-up-induced spalling

$P_{pore} > f_{ct}$

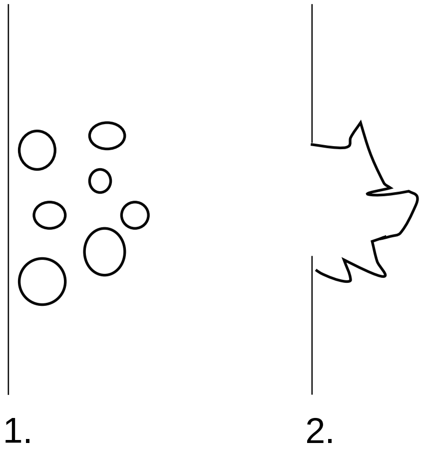

Figure 2. Spalling due to pore pressure

Thermal stress-induced spalling

$\sigma_{surface} > f_c$

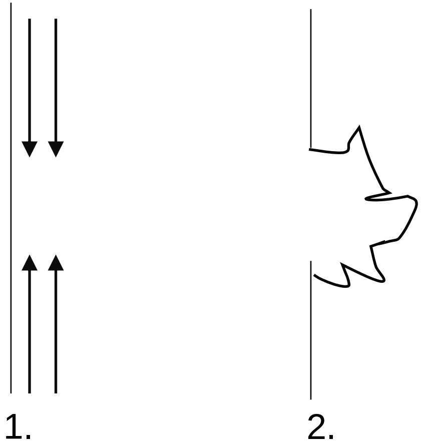

Figure 3. Spalling due to thermal stresses

1. Background

Factors affecting spalling behaviour:

- Porosity [1,2]
- Permeability [1,2]
- Moisture content [1,2,3]
- Aggregate size [4,5]
- Certain cement additives [6]
- Application of loading [6,7]
- Restraints [6,7]
- Size of the sample [8]

1. Background

Complexity of modelling concrete at elevated temperatures:

- Concrete is a porous, heterogeneous medium
- Presence of multi-phase water and associated phase changes
- Chemical reactions occurring in the cement (dehydration)
- Mechanical properties of concrete, reinforcing steel and water are temperature-dependent
- Many of the properties needed in the model equations are derived experimentally

1. Background

Modelling of concrete at elevated temperatures

- Despite micro scale heterogeneity, continuum assumption is valid
- Heterogeneity scale smaller than at which changes in temperature, moisture content or pressure can be observed [9]
- Different concretes characterized by macroscopic material properties despite micro scale differences [10]

1. Background

- Fire simulations commonly carried out using Fire Dynamics Simulator (FDS)
- In its current state, FDS lacks the functionality needed to model concrete spalling
- Aside from thermal conduction, a method to calculate moisture transfer in porous material is needed

1. Background

The objective: Expansion of FDS functionality and the existing solid thermal conduction solver into a coupled heat and mass transfer solver for porous materials

2. The model

2. The model

Modelling assumptions and simplifications

- 1D model
- Ideal gases
- Two phases: condensed (solid+liquid) and gas
- Movement of liquid water ignored
- Mechanical effects ignored
- Movement of gases described by Fick‘s law and Darcy‘s law
- Heat transfer via conduction only; thermal equilibrium; averaged thermal properties
- Phase changes and chemical reactions described by Arrhenius eqn.

2. The model

Primary variables

- Solid species mass fraction $Y_{s,\alpha}$
- Gas species mass fraction $Y_{g,\alpha}$
- Temperature T
- Pressure P

2. The model

$$Y_{\mathrm{s},\alpha} = \frac{m_{\mathrm{s},\alpha}}{m_{\mathrm{s}}} = \frac{X_{\mathrm{s},\alpha}\rho_{\mathrm{s},\alpha}}{\rho_{\mathrm{s}}},$$

$$\rho_{\mathrm{s}} = \left(\sum_{\alpha=1}^{N_{\mathrm{s}}} \frac{Y_{\mathrm{s},\alpha}}{\rho_{\mathrm{s},\alpha}}\right)^{-1},$$

$$\phi_\alpha = 1 - \sum_{\alpha=1}^{N_{\mathrm{s}}} \frac{\rho_{\mathrm{s},\alpha}}{\rho_{\mathrm{s,s},\alpha}},$$

$$\bar{\phi} = \sum_{\alpha=1}^{N_{\mathrm{s}}} X_{\mathrm{s},\alpha}\phi_\alpha$$

Solid phase preliminary definitions

$$Y_{\mathrm{g},\alpha} = \frac{m_{\mathrm{g},\alpha}}{m_{\mathrm{g}}} = \frac{X_{\mathrm{g},\alpha}\rho_{\mathrm{g},\alpha}}{\rho_{\mathrm{g}}},$$

$$\rho_{\mathrm{g}} = \frac{P\bar{M}}{RT},$$

$$\bar{M} = \left(\sum_{\alpha=1}^{N_{\mathrm{g}}} \frac{Y_{\mathrm{g},\alpha}}{M_\alpha}\right)^{-1}$$

Gas phase preliminary definitons

$$\rho = \rho_{\mathrm{s}} + \rho_{\mathrm{g}}.$$

Total density

2. The model

$$\frac{\partial(Y_{s,\alpha}\rho_s)}{\partial t} = \dot{\omega}'''_{s,\alpha}, \qquad 0 \leq x \leq L,$$

$$\frac{\partial(\overline{\phi}\rho_g)}{\partial t} = \frac{\partial}{\partial x}\left(\frac{K}{\bar{\nu}}\frac{\partial P}{\partial x}\right) + \dot{\omega}'''_{g,tot}, \qquad 0 \leq x \leq L,$$

$$\frac{\partial(\overline{\phi}Y_{g,\alpha}\rho_g)}{\partial t} = \frac{\partial}{\partial x}\left(Y_{g,\alpha}\frac{K}{\nu_\alpha}\frac{\partial P}{\partial x}\right) + \frac{\partial}{\partial x}\left(\overline{\phi}\rho_g D_\alpha \frac{\partial(Y_{g,\alpha})}{\partial x}\right) + \dot{\omega}'''_{g,\alpha}, \qquad 0 \leq x \leq L,$$

$$\frac{\partial(\rho\overline{c}T)}{\partial t} = \frac{\partial}{\partial x}\left(\overline{k}\frac{\partial T}{\partial x}\right) + \dot{q}''', \qquad 0 \leq x \leq L,$$

Governing equations

2. The model

Gas species boundary conditions

$$-\overline{\phi}\rho_{\mathrm{g}}D_{\alpha}\frac{\partial Y_{\mathrm{g},\alpha}}{\partial x} = \frac{h_1}{c_{\mathrm{g},\alpha}}\left(Y_{g,\alpha,\infty} - Y_{g,\alpha}\right) \qquad \text{at } x = 0,$$

$$\overline{\phi}\rho_{\mathrm{g}}D_{\alpha}\frac{\partial Y_{\mathrm{g},\alpha}}{\partial x} = \frac{h_2}{c_{\mathrm{g},\alpha}}\left(Y_{g,\alpha,\infty} - Y_{g,\alpha}\right) \qquad \text{at } x = L,$$

Pressure boundary conditions

$$P = P_{\infty} \qquad \text{at } x = 0,$$

$$P = P_{\infty} \qquad \text{at } x = L.$$

Heat transfer boundary conditions

$$-k\frac{\partial T}{\partial x} = \dot{q}_b'' \qquad \text{at } x = 0,$$

$$k\frac{\partial T}{\partial x} = \dot{q}_b'' \qquad \text{at } x = L,$$

3. The solver

3. The solver

Numerical solution, prototype

- Prototype programmed in MATLAB, later to be implemented in FDS
- Discretization using finite difference method
- Backward Euler scheme, fully implicit (later Crank-Nicolson)
- Iterative solver due to strong non-linearity
- Convergence checked with relative tolerance for mass fractions and absolute tolerance for other variables

3. The solver

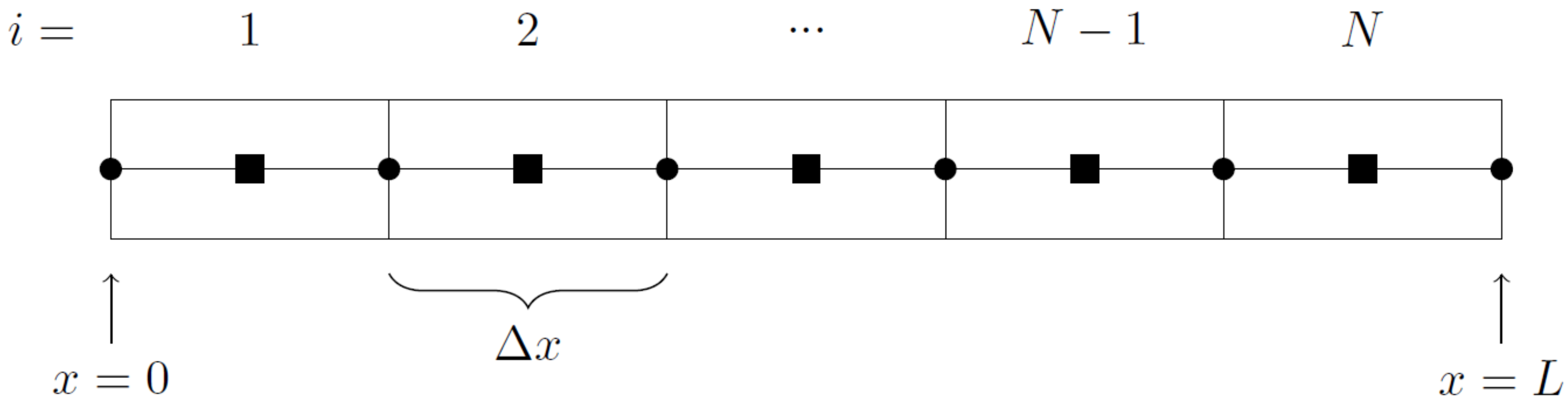

Figure 4. Discretization of the domain

3. The solver

Multiple problems have been encountered, and solved…

- First version, implicit Crank-Nicolson, but problems with source term splitting
- Second version, explicit Forward Euler, but instability due to trying to catch the acoustic pressure wave
- Third version, implicit Backward Euler, functional

… but there are still limitations and unfinished features

- Cannot account for swelling, shrinkage or removal of material (cells) yet
- Spalling too complex to be fully predictable in 1D…
- … but can be predicted with reasonable accuracy in 1D in certain scenarios relevant for tunnel fire simulation
- Crank-Nicolson scheme is still preferable to Backward Euler due to second vs. first order accuracy

3. The solver

Verification and validation

- Verification is being carried out
- Validation later using the results of planned small-scale experiments and data from literature

3. The solver

Transient heat conduction through a semi-infinite slab

- Four cases with varying parameters
- Comparison with analytical solution and FDS

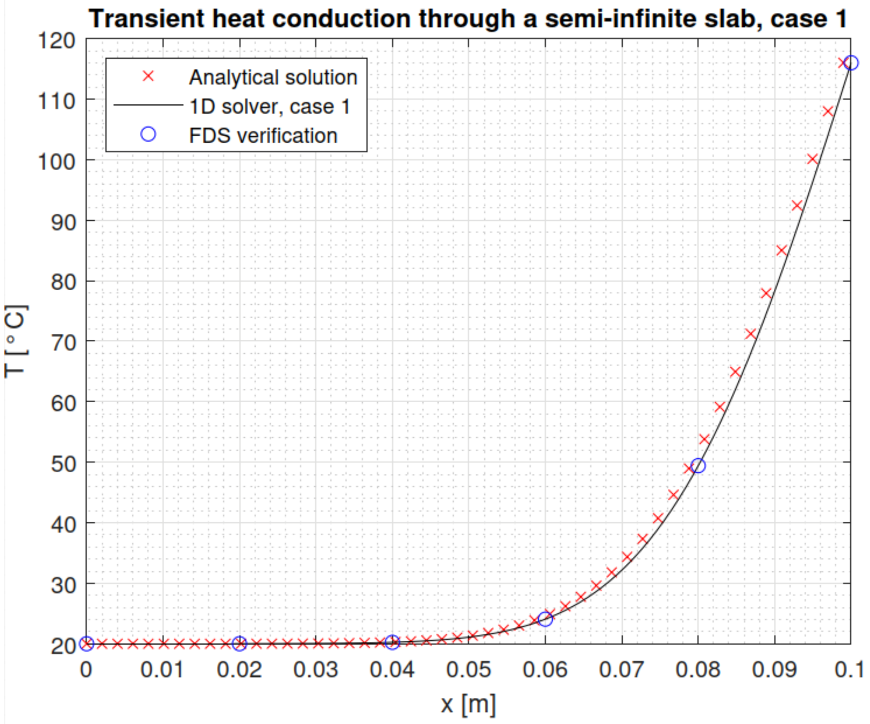

Figure 5. Transient heat conduction through a semi-infinite slab, analytical vs. numerical solution

3. The solver

Gas phase mass conservation, sealed system

- Sealed front and back surface
- Source term activates, releases a set amount of gas into system for a given time, then deactivates

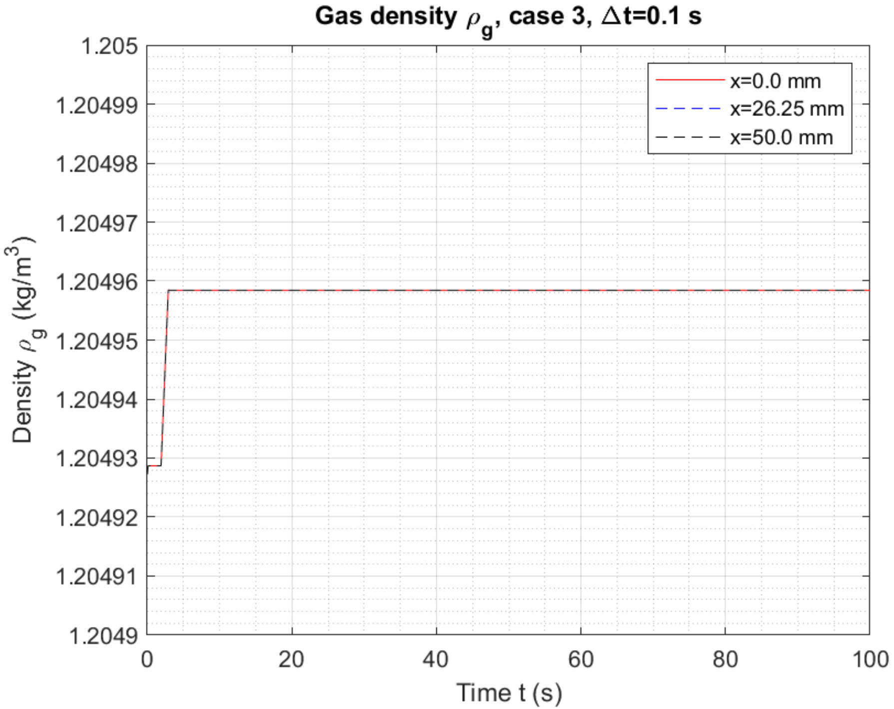

Figure 6. Gas phase mass conservation, sealed system

Aalto-yliopisto
Insinööritieteiden korkeakoulu

3. The solver

Gas phase mass conservation, mass flux through back

- Sealed front, open back surface
- Gas concentration (and pressure) spike / excess mass at t=0 s in the first cell

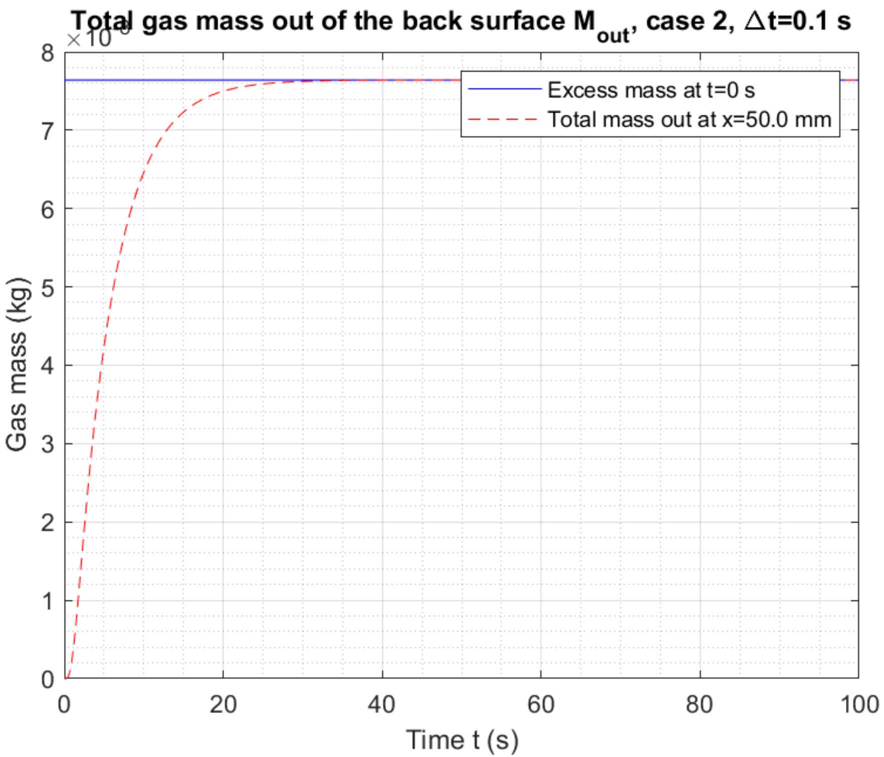

Figure 7. Gas phase mass conservation, mass flux through back surface

References

1. Mindeguia JC., Carré H., Pimienta P., La Borderie C. Experimental discussion on the mechanisms behind the fire spalling of concrete. Fire and Materials. 2015;39(7):619-635.
2. Maier M., Zeiml M., Lackner R. On the effect of pore-space properties and water saturation on explosive spalling of fire-loaded concrete. Construction and Building Materials. 2020;231.
3. Kirchhof LD., Lima RCA., Neto ABSS., Quispe AC., Filho LCOS. Effect of Moisture content on the behavior of high strength concrete at high temperatures [Efeito do teor de umidade no comportamento do concreto de alta resistência em altas temperaturas]. Revista Materia. 2020;25(1).
4. Pan Z., Sanjayan JG., Kong DLY. Effect of aggregate size on spalling of geopolymer and Portland cement concretes subjected to elevated temperatures. Construction and Building Materials. 2012;36:365-372.
5. Jansson R., Boström L. Experimental study of the influence of polypropylene fibres on material properties and fire spalling of concrete. In: Proceedings from the fib Task Group 4.3 workshop “Fire Design of Concrete Structures – From Materials Modelling to Structural Performance"; 2007. p. 177-88.
6. Hertz KD. Limits of spalling of fire-exposed concrete. Fire Safety Journal. 2003;38(2):103-116.
7. Jansson R. Fire Spalling of Concrete. Theoretical and Experimental Studies. KTH Architecture and the Built Environment. Stockholm, Sweden; 2013.
8. Mohd Ali AZ., Sanjayan J., Guerrieri M. Specimens size, aggregate size, and aggregate type effect on spalling of concrete in fire. Fire and Materials. 2018;42(1):59-68
9. Dwaikat MB., Kodur VKR. Hydrothermal model for predicting fire-induced spalling in concrete structural systems. Fire Safety Journal. 2009;44(3):425-434
10. Zhang Y., Zeiml M., Maier M., Yuan Y., Lackner R. Fast assessing spalling risk of tunnel linings under RABT fire: From a coupled thermo-hydro-chemo-mechanical model towards an estimation method. Engineering Structures. 2017;142:1-19

Thank you!

aalto.fi

Aalto-yliopisto
Insinööritieteiden
korkeakoulu